The Need for a Large-Scale Dense Array of Ground Based Observatories to Monitor Thermospheric and Space Weather

Primary Author: Mark G. Conde¹

Contributing Authors: D. L. Hampton¹, D. Thorsen¹, A. J Ridley², W. A Bristow³, B. J. Harding⁴, M. S. Dhadly⁵, R. Mesquita⁶, P. Dandenault⁶, F. Banks⁷, J. J. Makela⁸, A. Bhatt⁹, E. Kendall⁹, M. Taylor¹⁰, C. R. Martinis¹¹, W. Rideout¹², J. Chau¹³, S. Datta-Barua¹⁴, E. Donovan¹⁵, E. Spanswick¹⁵

<u>1:</u> Geophysical Institute, University of Alaska Fairbanks; <u>2:</u> University of Michigan, <u>3:</u> Penn State University, <u>4:</u> Space Sciences Laboratory, University of California Berkeley; <u>5:</u> US Naval Research Laboratory; <u>6:</u> Johns Hopkins University Applied Physics Laboratory; <u>7:</u> Battelle Memorial Institute; <u>8:</u> Department of Electrical and Computer Engineering, University of Illinois Urbana-Champaign; <u>9:</u> SRI International; <u>10:</u> Utah State University; <u>11:</u> Boston University; <u>12:</u> Massachusetts Institute of Technology; <u>13:</u> IAP Germany; <u>14:</u> Illinois Institute of Technology; <u>15:</u> University of Calgary.

Synopsis:

Each year, society becomes ever more reliant on spacecraft in low Earth orbit, and on systems that transmit radio signals through Earth's ionosphere. However, both spacecraft orbits and radio propagation are strongly affected by natural variations or "weather" occurring in the height range from ~80 km to several hundred kilometers altitude – the so-called "Space Atmosphere Interaction Region" (SAIR). Weather in this region is described by a coupled system of three-dimensional time-dependent partial differential equations that can only be evaluated using numerical models, which are limited because: (1) available computational resources only allow coarse grid resolutions, (2) solutions require specifications of drivers and boundary conditions that are not adequately described by observations, and (3) accurate evaluation of some terms may not be computationally feasible. These limitations create an urgent need for comprehensive real-time observations of the actual state of the SAIR, and the drivers of its weather – to constrain the models, to validate their physics, and to provide timely, actionable data to end-users of technological systems. Unfortunately, however, existing infrastructure for observing SAIR weather is astonishingly inadequate. For example, even as early as the mid-1800s, routine meteorological observations of the troposphere had already exceeded today's typical resolution for the corresponding measurements in the SAIR. The proposed solution is to establish a large array of roughly thirty relocatable ground-based flagship observatories, and a similar number of simpler and lower-cost instrument outposts. These would be deployed from the Canadian arctic down through the Americas to southern Argentina, with observational coverage spanning SAIR altitudes. Observatory instruments would characterize winds, temperatures and electrodynamics within the SAIR, as well as the drivers that force these fields – both from above, due to solar radiation and geomagnetic activity, and from below, due to upward propagating waves and tides. Cyber infrastructure would be developed to host and freely distribute observational data, assimilate observations contributed by others, and provide higher-level data products derived from assimilation and modeling. The array of observatories proposed here is essentially an exact realization of one of the major recommendations of the previous (2013) Heliophysics Decadal Survey, that has yet to be implemented.

1.1 Background Physics

Over altitudes in Earth's atmosphere between about 90 and several hundred km the governing physics transitions from neutral fluid dynamics in the lower atmosphere to plasma electrodynamics in the geospace region above. This Space-Atmosphere Interaction Region (SAIR) strongly impacts modern technological systems [National Space Weather Plan, 2015]. Its ionized component controls radio wave propagation, and so affects communication, navigation, and long-range radar. Density, pressure, and winds of its neutral component affect spacecraft orbits, with high dollar-value consequences for predictions of orbital reentries and for collision avoidance maneuvers. Mitigating these effects requires that the SAIR can be observed in real-time, and forecast into the near-term future.

The SAIR's neutral and ionized components are subject to external forcing via solar ultraviolet radiation, electrodynamic drivers from the solar wind interacting with Earth's magnetosphere (i.e. electric fields and auroral precipitation), and by waves and tides propagating up from the middle and lower atmosphere, to drive winds that in turn force plasma motion and can trigger internal instabilities [Chau et al. 2012; Pautet et al., 2016.] The balance among these various drivers depends on meteorological activity in the lower atmosphere, and conditions in the space environment due to solar and magnetospheric activity. The response to these drivers is governed by a coupled system of three-dimensional time-dependent partial differential equations [e.g. see Ridley et al., 2006]. Dominant terms in these equations involve partial derivatives with respect to the all three spatial coordinates, and time. To take one very simple example, there is an absolute requirement for conservation of mass, which is expressed via the equation of mass continuity as

$$\frac{\partial \rho}{\partial t} + \nabla \cdot (\rho \, \overrightarrow{\mathbf{u}}) = \sigma$$
 where
$$\begin{cases} \rho = \text{ mass density} \\ \overrightarrow{\mathbf{u}} = \text{ flow velocity} \\ \sigma = \text{ source/sink term for mass - usually zero} \end{cases}$$

This equation is strongly dependent on derivatives of mass flux with respect to each spatial coordinate variable, and on the time derivative of mass density. Other relevant equations include those for conservation of energy and momentum, and rates of change of chemical composition, for both neutral and ionized species – all of which also include strong dependencies on spatial and temporal derivatives. Complete understanding of the dynamical state of the SAIR would thus require observations of all relevant parameter fields over an extended region in space and time, and with sufficient spatial, temporal, and measurement resolution to allow all derivative terms to be evaluated, down to the shortest significant spatial and temporal scales.

1.2 Observational Shortcomings

Unfortunately, currently deployed observational assets fall (very) far short of providing such a full observational characterization of the SAIR, and achieving this goal is far beyond any practical upgrades that could be implemented over the next decade, or beyond. Instead, the purpose of this White Paper is to consider whether it would be feasible to upgrade the network of SAIR observatories enough to detect new regimes of behavior, as a result of improved resolution of spatial and temporal structure.

Of course, existing instrumentation spans an enormous diversity of measurement techniques, target parameters, instrument locations (including ground versus spacebased), and measurement dimensionality. Many parameters are already measured frequently from numerous ground and space-based platforms. While some (such as ionospheric total electron content) are routinely mapped in two dimensions, many quantities are only observed through single-point measurements taken as a function of time. For ground-based instruments this gives the measurement parameter's time history, but only at the instrument location. For spacecraft sensors, single-point measurements define the parameter values along the orbit, but not elsewhere, and they do not allow construction of the time history at a fixed location. In either case, single-point measurements only capture variations along one dimension. The result is a sparse "cut" through the SAIR, whose parameter fields actually vary across four dimensions: lon-

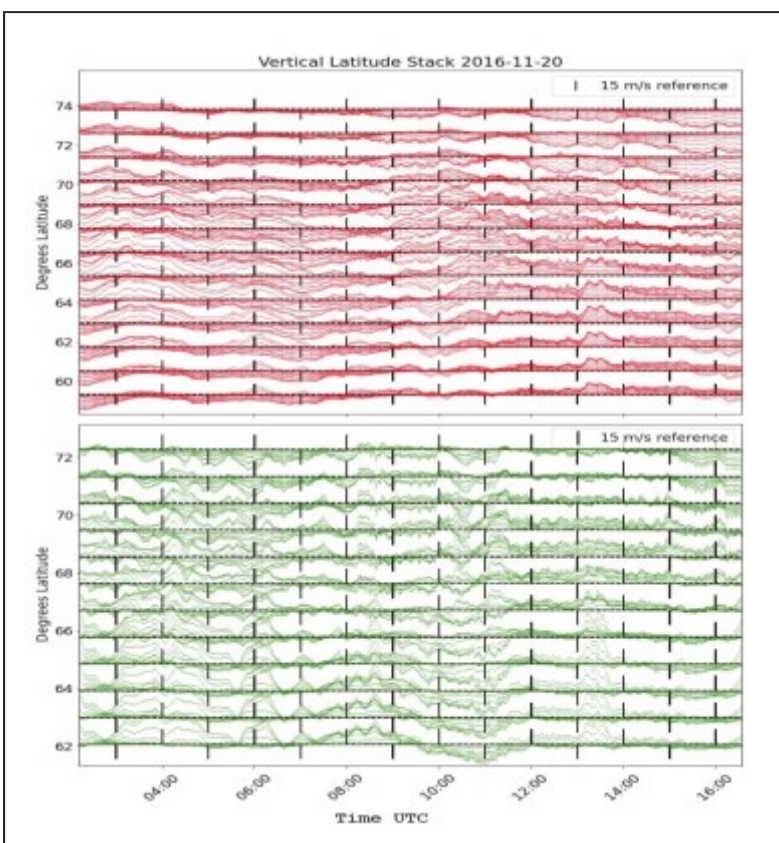


Figure 1: Vertical wind as a function of time and geographic latitude, at altitudes of 240 km (red) and 120 km (green), derived from line-of-sight wind components measured using four all-sky imaging Fabry-Perot spectrometers deployed across Alaska. Multiple traces appear at each latitude because winds were also measured at multiple longitudes. (Adapted from *Elliott & Conde*, 2022.)

gitude, latitude, altitude, and time. A further problem is that almost all SAIR parameters vary far more rapidly with height than they do in either horizontal direction, yet height is the SAIR dimension that is least well sampled.

1.3 Phenomena Not Captured by Current Instrumentation

There are innumerable and urgent problems in SAIR physics for which a modest improvement over existing sampling resolution would greatly improve current understanding. These include, but are <u>not limited</u> to:

1. **The spatial distribution of SAIR vertical winds**. The limited number of existing studies of the geographic distribution of vertical winds in Earth's thermosphere suggests these winds vary strongly over horizontal scales as short as a few hundred kilometers or less [McLeod, 1968; Ishii et al., 2004; Anderson et al., 2011; Anderson et al., 2012; Larsen &

Meriwether, 2012; Conde et al., 2018; Elliott & Conde, 2022.] Figure 1 illustrates this variability, at least across a small region corresponding to the main body of Alaska. Vertical wind transport is known to modify thermospheric [O]/N2], whereas horizontal winds transport these perturbations globally [e.g. Prolss [1997.] Understanding and modeling of this important process must account for the geographic variability of vertical wind.

2. The scale size of thermospheric weather systems. As shown in Figure 2 [Harding, pers comm 2019], current instrumentation cannot even resolve the large-scale distribution of scale sizes of thermospheric wind systems.

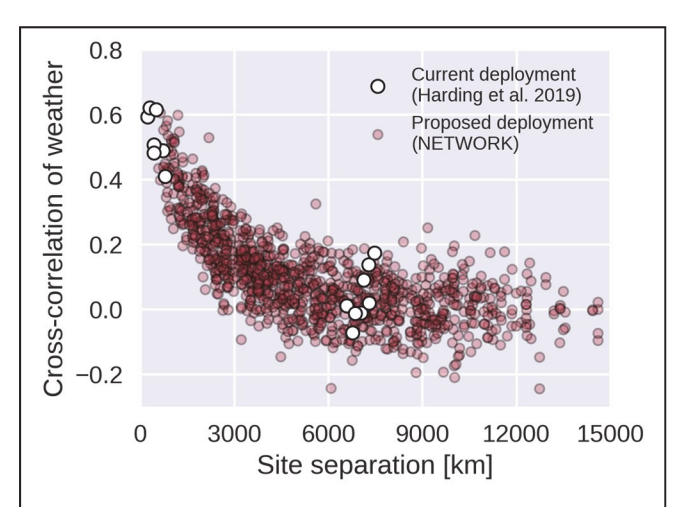


Figure 2: Correlation between F-region winds, as a function of the separation between the measurement sites, as discussed in the main te_xt.

The figure shows the correlation between winds measured at pairs of locations, as a function of separation distance between the two measurements. White markers show *Harding et al.* [2019] results using one year of data from an existing array of instruments deployed at seven sites in North and South America. Existing instruments can only show that nearby sites (< 1000 km) exhibit correlated weather, while distant sites (>6000 km) do not. Red markers predict the far greater resolution that would be possible using the network of observatories proposed here, based on an assumed wind model sampled at the locations shown in Figure 4.

3. **Transport of SAIR air masses by horizontal winds.** Trajectories of air masses transported by winds can be extremely complicated, even in the thermosphere, where the wind field is far smoother than its tropospheric counterpart. This complexity is illustrated in Figure 3, adapted from *Dhadly & Conde* [2017.] The colored traces show trajectories of air parcels traced backward in time through the F-region wind field observed above Alaska

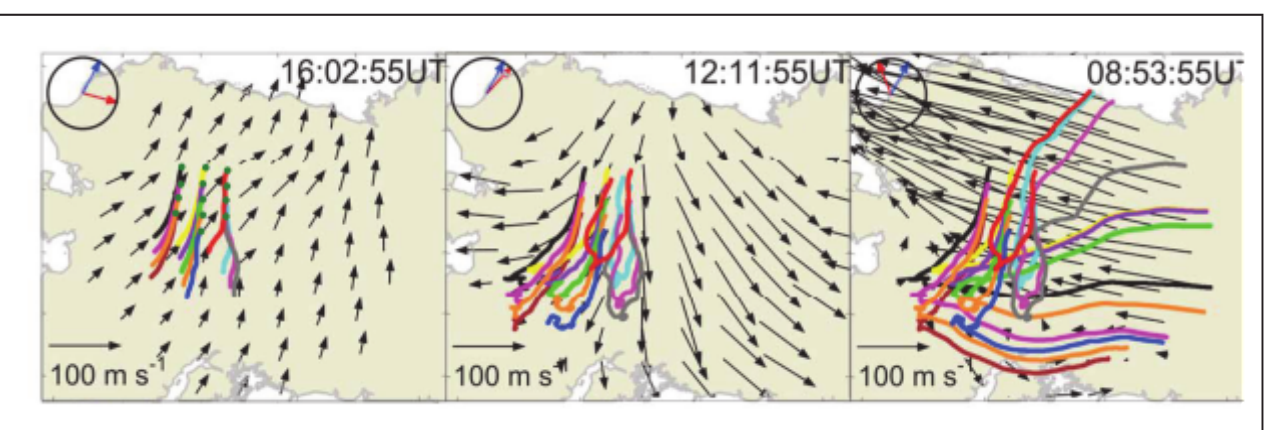


Figure 3: The left panel depicts, using green dots, a compact array of 13 locations. Each panel shows the prior trajectories of air parcels that arrived over these locations at 17:41 UT. The three panels show trajectories traced back to 16:03 UT (left), 12:13 UT (middle), and 08:54 UT (right).

over many hours. They show the past trajectories of air masses that passed over a compact grid of 13 locations (~90 km grid spacing) at 17:41 UT. The three panels show the prior trajectories of these air parcels beginning at three earlier times. While these air parcels were very close to each other at 17:41 UT, the 08:53:55 UT panel shows that they had very different prior histories and originated from very different source regions.

4. Local-scale ion-neutral momentum coupling. Analysis of neutral winds and ion drifts measured by the DE-2 satellite in the 1980s suggested that the time-constant for ion-neutral momentum coupling in Earth's

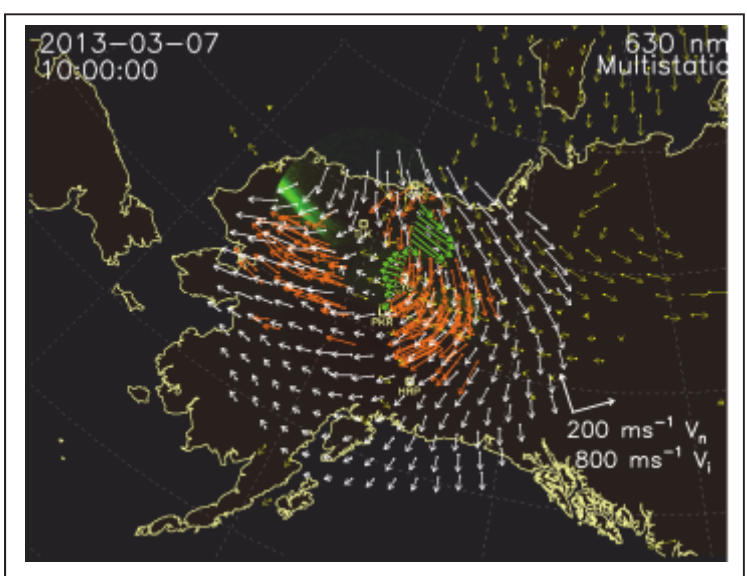


Figure 4: F-region ionospheric drifts measured by the SuperDARN (yellow arrows) and PFISR (green arrows) radars, overlaid onto F-region neutral winds (white & orange arrows) measured using Fabry-Perot spectrometers. Note how the neutral flow pattern mimics that of the ions.

thermosphere is typically one to several hours [e.g. *Killeen et al.*, 1984,1985; *Ponthieu et al.*, 1988.] This, in turn, led to an expectation that ion motion could only influence the neutral wind at synoptic scales or larger. However, *Kosch et al.* [2001] showed that this time constant could, at times, be much less than an hour, whereas *Conde et al.* [2018] showed that the F-region neutral wind field could respond to ion drifts on much shorter length & time scales: 100 to 200 km spatially, and ~15 minutes temporally. Figure 4 presents one example of this. However, the morphology of this small-scale ion-neutral coupling is currently not well explored. The extended array of instruments proposed here would greatly improve understanding of this coupling regime, by providing high resolution measurements of flows and background properties for both the thermosphere and ionosphere.

5. **Gravity waves in the SAIR.** Gravity waves are commonly observed in the Earth's thermosphere [e.g., *Hocke et al.*, 1996; *Oliver et al.*, 1997; *Djuth et al.*, 1997, 2004; *Yiğit & Medvedev*, 2012; *England et al.*, 2020.] Thermospheric GWs can either be generated in-situ by geomagnetic activity [e.g. *Oyama et al.*, 2001], or can result from dissipation and breaking of waves propagating upward from lower atmospheric layers [*Fritts & Alexander*, 2003; *Vadas & Fritts*, 2006.] With horizontal wavelengths of a few hundred kilometers or more, and intrinsic periods ranging from ~15 minutes to several hours, the underlying wind and temperature perturbations associated with such waves could be resolved far better than is currently possible using instrument array proposed here.

We propose that the science topics described above (and many others) could be addressed by an ambitious set of new SAIR observatories deployed throughout North and South America. The concept presented here was actually proposed to NSF in 2019 in response to their "Mid-Scale



Figure 5: Fields of view (FoV) of the proposed observatories & instruments. Pink and green circles (projection distorted) indicate ground-based cameras imaging at 630 nm and 558 nm; four red dots indicate narrow-field FPI sampling; lilac circles denote SDI FoV; blue wedges show Super-DARN FoV; orange/green shadings denote the multistatic meteor radars FoV; and dashed contours show magnetic latitude.

Research Infrastructure" solicitation. It was not selected – which is unsurprising given that only a small number of projects were funded across <u>all</u> the disciplines supported by NSF. Nevertheless, it was clear from the enthusiastic reviews that the heliophysics community would be well served by continuing to push for a capability similar to this.

As shown in Figure 5, the proposed observatory network would consist of approximately 30 flagship observatory sites, supported by a similar number of simpler instrument outposts. The array would extend from Thule, Greenland, running down through Canada and the Americas to southern Argentina, with observational coverage spanning altitudes from ~80 to several hundred kilometers. It would span most geomagnetically relevant latitudes.

Observatory instruments would characterize winds, temperatures and electrodynamics within the thermosphere and ionosphere, as well as the drivers from above and below. A baseline suite of instruments to be deployed is shown in Table 1, along with their corresponding measurement characteristics. We emphasize, however, that the observatories would be established as general purpose facilities. Many other instruments could be accommodated either in addition to, or in place of, the baseline suite. The observatory buildings and instruments within would use existing, proven designs and providers with field experience, allowing for a low-risk, "shovel ready" project.

Instrument/Parameter	Field-of-View	Typical Resolution	Uncertainty
SDI/wind & temp @ h=120 km	Circular, Ø750 km	H:60 km, t:2-20 min	±5m/s;±10K
SDI/wind & temp @ h=240 km	Circular, Ø1400 km	H:115 km, t:2-20 min	±5m/s;±20K
FPI/wind & temp @ h=240 km	NESW @ 45°	H:500 km, t:2-30 min	±5m/s;±15K
All-Sky Imager/840 nm intensity	Circular, ø520 km	H:2km, t:10 sec	±1% relative
All-Sky Imager/558 nm intensity	Circular, Ø600 km	H:2km, t:10-240 sec	±1% relative
All-Sky Imager/630 nm intensity	Circular, Ø1400 km	H:2-4km, t:10-240 sec	±1% relative
All-Sky Imager/589 nm intensity	Circular, Ø600 km	H:2km, t:10-240 sec	±1% relative
AMTM/Temperature @ h=87 km	Rectangular,180×144km	H:600 m, t:30 sec	±2K
SuperDARN/Plasma velocity	Fan, 54°×3599 km	H:45 km, t:2 min	±45
SIMO/Winds @ h=80-100 km	Circular, Ø400 km	V:2km, t:1 hour	±2km
MIMO/Winds @ h=80-100 km	Elongated, 400×2400km	H:15km,V:1km,t:30min	±15k
GNSS RX/TEC, Scintillations	Circular, 150° full-angle	t:1Hz TEC; 50Hz Scint	±1%
Magnetometer, B-field variations	Local	t:1 sec	±1nT
Ionosonde/Elec Den @80-400km	Vertical Profile	t:15 min	Varies

Table 1: Baseline instruments and measurement characteristics. SDI: Scanning (all sky) Doppler Imager [*Dhadly & Conde*, 2016; *Conde et al.*, 2018]; FPI: Fabry-Perot Interferometer [*Makela et al.*, 2009, 2011, 2012; *Zhang et al.*, 2013; *Harding et al.*, 2014, 2015; *Chartier et al.*, 2015]; AMTM: Advanced Mesospheric Temperature Mapper [*Fritts et al.*, 2014; Pendelton et al., 2014; *Negale et al.*, 2018]; SIMO: monostatic mesospheric meteor radar; MIMO: Multistatic meteor radar [*Chau et al.*, 2017, 2018; *Vierinen et al.*, 2016, 2019]; GNSS: Global Navigation Satellite System; TEC: ionospheric Total Electron Content [*Zou et al.*, 2013].

Flagship observatories would be based on customized 8'×20' shipping containers, as shown in Figure 6. Outposts will be simpler 8'×8' enclosures. Both are available from US vendors. They would be fitted for human occupancy, with insulation and climate control for both arctic and tropical conditions, and configured for easy transport by sea, road, or rail. Specific instruments deployed at each site will be determined by (1) the relative importance of the various drivers affecting the SAIR at that geographic location, and (2) avoiding duplication of existing nearby instruments with similar capabilities. The observatories are designed to be easily relocatable should the need arise during the life of this project. Monte-Carlo simulations indicate that 50% of the time, 72% of the proposed sites will either be clear or at most partly cloudy.

These observatories would build on the prior success of smaller ionospheric sensor arrays, such as SuperDARN, GNSS, and regional optical networks in North and South America [Bust et al., 2007; Zou et al., 2013; Martinis et al., 2018; and Lyons et al., 2019.] However, it would vastly extend both the geographic coverage and physical domain of the measurements, and address the full gamut of fundamental research spanning the middle atmosphere, through the SAIR, and up into the magnetosphere. It would determine the roles of and balance between upward and downward energy and momentum forcing of weather in the SAIR region. The multitude of parameters

measured simultaneously at so many locations would impose far tighter constraints on the state of the SAIR than would arise if "system knowledge" simply scaled linearly with the number of measurements. It would revolutionize our instrumental view of the SAIR and, for the first time, enable characterization of the multi-scale SAIR state evolving across longitude, latitude, altitude, and time.

3. Urgency of Need for the Proposed Infrastructure

The pressing need for this capability has been identified in a series of Geospace Science community planning documents, including the previous *Decadal Survey for Solar and Space Physics*

[2013], the National Space Weather Action Plan [2015], and the NSF Portfolio Review of the Geospace Section of the Division of Atmospheric and Geospace Science [NSF, 2016]. In particular, the previous 2013 Decadal Survey noted that: "Processes central to AIM [Atmosphere-Ionosphere-Magneto-sphere] science are multiscale in nature, with global features that extend from the equator to the poles together with local features such as embedded small-scale irregularities that intermittently affect communications." To characterize these processes, the 2013 Decadal Survey recommended that the Heliophysics community should:

"Develop, deploy, and operate a network of 40 or more autonomous observing stations extending from pole to pole through the (North and South) American longitudinal sector. The network nodes should be populated with heterogeneous instrumentation capable of measurements including winds, temperatures, emissions, scintillations, and plasma parameters, for study of a variety of local and regional ionosphere-thermosphere phenomena over extended latitudinal ranges."



Figure 6: A container lab under construction in July 2022.

Given this strong prior recommendation, together with the Heliophysics community's need to support the forthcoming GDC and DYNAMIC missions, it is expected that other white papers may be submitted suggesting comparable efforts. If so, this would strongly demonstrate the wide community support for an extended network of ground-based SAIR monitoring observatories.

4. Implementation

The deployment proposed here would involve numerous technical, logistic, and regulatory tasks that would require a dedicated Science Support contractor. NSF has worked previously with various contractors to create similar large networks – such as EarthScope or NEON. Lessons learned from these projects would be available to guide this project. Also, the previous NSF proposal did develop plans for implementation, including the observatory design and fabrication, scalability of base units, site permitting, environmental & cultural impacts, logistics to ship, install, & commission the observatories and instruments, maintenance & management of spares, required cyber-infrastructure, collaboration with partners and end-users, and overall project management. Numerous beneficial broader impacts were also identified. Once established, operation and maintenance of the network would be supported similarly to other NSF large-scale facilities.

- Anderson, C., Davies, T., Conde, M., Dyson, P. and Kosch, M.J., 2011. Spatial sampling of the thermospheric vertical wind field at auroral latitudes. *Journal of Geophysical Research: Space Physics*, 116(A6).
- Anderson, C., Conde, M. and McHarg, M.G., 2012. Neutral thermospheric dynamics observed with two scanning Doppler imagers: 2. Vertical winds. *Journal of Geophysical Research: Space Physics*, 117(A3).
- Bust, G. S., G. Crowley, T. W. Garner, T. L. Gaussiran II, R. W. Meggs, C. N. Mitchell, P. S. J. Spencer, P. Yin, and B. Zapfe, 2007. Four-dimensional GPS imaging of space weather storms, *Space Weather*, 5, S02003, doi:10.1029/2006SW000237.
- Chartier, A.T., J.J. Makela, H. Liu, G.S. Bust, and J. Noto, 2015. Modeled and observed equatorial thermospheric winds and temperatures, *J. Geophys. Res. Space Physics*, 120, 5832–5844.
- Chau, J. L., L. P. Goncharenko, B. G. Fejer, and H. L. Liu, 2012. Equatorial and Low Latitude Ionospheric Effects During Sudden Stratospheric Warming Events Ionospheric Effects During SSW Events, *Space Science Reviews*, 168, 1-4, pp 385-417, DOI: 10.1007/s11214-011-9797-5.
- Chau, J. L., G. Stober, C. Hall, M. Tsutsumi, F. I. Laskar, and P. Hoffmann, 2017. Polar mesospheric horizontal divergence and relative vorticity measurements using multiple specular meteor radars, *Radio Sci.*, 52, doi:10.1002/2016RS006225.
- Chau, J. L., J. M. Urco, J. P. Vierinen, R. A. Volz, M. Clahsen, N. Pfeffer, and J. Trautner, 2018. Novel specular meteor radar systems using coherent MIMO techniques to study the mesosphere and lower thermosphere, *Atmos. Meas. Tech. Discuss.*, https://doi.org/10.5194/amt-2018-287.
- Committee on a Decadal Strategy for Solar and Space Physics (Heliophysics) 2013. *Solar and Space Physics, A Science for a Technological Society*, The National Academies Press, Washington DC.
- Conde, M.G., Bristow, W.A., Hampton, D.L. and Elliott, J., 2018. Multi-instrument studies of thermospheric weather above Alaska. *Journal of Geophysical Research: Space Physics*, 123(11), pp.9836-9861.
- Conde, M.G., W.A. Bristow, D.L. Hampton, and J. Elliott, 2018. Multi-instrument studies of thermospheric weather above Alaska, *J. Geophys. Res.* 123. https://doi.org/10.1029/2018JA025806
- Dhadly, M.S. and Conde, M., 2016. Distortion of thermospheric air masses by horizontal neutral winds over Poker Flat Alaska measured using an all-sky scanning Doppler imager. *Journal of Geophysical Research: Space Physics*, 121, 854–866, doi:10.1002/2015JA021800.
- Dhadly, M. and Conde, M., 2017. Trajectories of thermospheric air parcels flowing over Alaska, reconstructed from ground-based wind measurements. *Journal of Geophysical Research: Space Physics*, 122(6), pp.6635-6651.
- Djuth, F.T., Sulzer, M.P., Elder, J.H. and Wickwar, V.B., 1997. High-resolution studies of atmosphere-ionosphere coupling at Arecibo Observatory, Puerto Rico. *Radio Science*, *32*(6), pp.2321-2344.

- Djuth, F.T., Sulzer, M.P., Gonzales, S.A., Mathews, J.D., Elder, J.H. and Walterscheid, R.L., 2004. A continuum of gravity waves in the Arecibo thermosphere? *Geophysical Research Letters*, 31(16).
- Elliott, J. and Conde, M.G., 2022. High Spatial and Temporal Resolution Studies of Thermospheric Vector Wind Fields Derived From a Ground-Based Network of All-Sky Fabry-Perot Interferometers. *Journal of Geophysical Research: Space Physics*, 127(8), p.e2022JA030481.
- England, S.L., Greer, K.R., Solomon, S.C., Eastes, R.W., McClintock, W.E. and Burns, A.G., 2020. Observation of thermospheric gravity waves in the southern hemisphere with GOLD. *Journal of Geophysical Research: Space Physics*, 125(4), p.e2019JA027405.
- Fritts D.C., Pautet P.-D., Bossert K., Taylor M.J., Williams B.P., Iimura H., Yuan T., Mitchell N.J., and Stober G., 2014. Quantifying gravity wave momentum fluxes with mesosphere temperature mappers and correlative instrumentation, *J. Geophys. Res.*, 119, Issue 24, 13583-13603, doi: 10.1002/2014JD022150.
- Harding, B. J., T. W. Gehrels, and J. J. Makela, 2014. Nonlinear regression method for estimating neutral wind and temperature from Fabry–Perot interferometer data, *Appl. Opt.*, 53(4), 666.
- Harding, B. J., J. J. Makela, and J. W. Meriwether, 2015. Estimation of mesoscale thermospheric wind structure using a network of interferometers, *J. Geophys. Res. Space Physics*, 120, 3928–3940.
- Harding, B.J., Ridley, A.J. and Makela, J.J., 2019. Thermospheric weather as observed by ground-based FPIs and modeled by GITM. *Journal of Geophysical Research: Space Physics*, 124(2), pp.1307-1316.
- Hocke, K. and Schlegel, K., 1996. A review of atmospheric gravity waves and travelling ionospheric disturbances: 1982–1995. In *Annales Geophysicae* (Vol. 14, No. 9, p. 917).
- Ishii, M., Kubota, M., Conde, M., Smith, R.W. and Krynicki, M., 2004. Vertical wind distribution in the polar thermosphere during Horizontal E Region Experiment (HEX) campaign. *Journal of Geophysical Research: Space Physics*, 109(A12).
- Killeen, T.L., Hays, P.B., Carignan, G.R., Heelis, R.A., Hanson, W.B., Spencer, N.W. and Brace, L.H., 1984. Ion-neutral coupling in the high-latitude F region: Evaluation of ion heating terms from Dynamics Explorer 2. *Journal of Geophysical Research: Space Physics*, 89(A9), pp.7495-7508.
- Killeen, T.L., Heelis, R.A., Hays, P.B., Spencer, N.W. and Hanson, W.B., 1985. Neutral motions in the polar thermosphere for northward interplanetary magnetic field. *Geophysical research letters*, 12(4), pp.159-162.
- Kosch, M.J., Cierpka, K., Rietveld, M.T., Hagfors, T. and Schlegel, K., 2001. High-latitude ground-based observations of the thermospheric ion-drag time constant. *Geophysical research letters*, 28(7), pp.1395-1398.
- Larsen, M.F. and Meriwether, J.W., 2012. Vertical winds in the thermosphere. *Journal of Geophysical Research: Space Physics*, 117(A9).

- Lyons, L., Y. Nishimura, S.-R. Zhang, A. J. Coster, A. Bhatt, E. Kendall, and Y. Deng, 2019. Identification of Auroral Zone Activity Driving Large-Scale Traveling Ionospheric Disturbances, *J. Geophys. Res.*, Vol 124, No. 1, doi:10.1029/2018JA025980
- MacLeod, M. A. (1968), Vertical neutral winds from chemical releases, in Meteorological and Chemical Factors in D-Region Aeronomy: Record of the Third Aeronomy Conference, Aeron. Rep., 32, pp. 142–159, Aeron. Lab., Univ. of Ill., Urbana-Champaign.
- Makela, J. J., J. W. Meriwether, J. P. Lima, E. S. Miller, and S. J. Armstrong, 2009. The Remote Equatorial Nighttime Observatory of Ionospheric Regions Project and the International Heliospherical Year, *Earth Moon Planets*, 104(1-4).
- Makela, J. J., J. W. Meriwether, Y. Huang, and P. J. Sherwood, 2011. Simulation and analysis of a multi-order imaging Fabry–Perot interferometer for the study of thermospheric winds and temperatures, *Appl. Opt.*, 50(22), 4403-4416.
- Makela, J. J., J. W. Meriwether, A. J. Ridley, M. Ciocca, and M. W. Castelaz, 2012. Large-Scale Measurements of Thermospheric Dynamics with a Multisite Fabry-Perot Interferometer Network: Overview of Plans and Results from Midlatitude Measurements, Int. *J. Geophys.*, 2012, Article ID 872140.
- Martinis, C., J. Baumgardner, J. Wroten, M. Mendillo, 2018. All-sky-imaging capabilities for ionospheric space weather research using geomagnetic conjugate point observing sites, *Advances in Space Research*, 61, Issue 7.
- National Science and Technology Council, 2015. National Space Weather Plan.
- Negale, M.R., M.J. Taylor, M.J. Nicolls, S.L Vadas, K. Nielsen, and C.J. Heinselman, 2018. Seasonal propagation characteristics of MSTIDs observed at high latitudes over central Alaska using the Poker Flat Incoherent Scatter Radar, *J. Geophys. Res.: Space Phys.*, 123, 5717-5737, doi: 10.1029/2017JA024876.
- NSF Portfolio Review Committee, *Investments in Critical Capabilities for Geo-space Science* 2016 to 2025: Portfolio Review of the Geospace Section of the Division of Atmospheric and Geospace Science, 2016.
- Oliver, W.L., Otsuka, Y., Sato, M., Takami, T. and Fukao, S., 1997. A climatology of F region gravity wave propagation over the middle and upper atmosphere radar (Paper 97JA00491). *Journal of Geophysical Research*, 102, pp.14-499.
- Oyama, S., Ishii, M., Murayama, Y., Shinagawa, H., Buchert, S.C., Fujii, R. and Kofman, W., 2001. Generation of atmospheric gravity waves associated with auroral activity in the polar F region. *Journal of Geophysical Research: Space Physics*, 106(A9), pp.18543-18554.
- Pautet P.-D., Taylor M.J., Fritts D.C., Bossert K., Williams B.P., Broutman D., Ma J., Eckermann S., and Doyle J. 2016. Large amplitude mesospheric response to an orographic wave generated over the Southern Ocean Auckland Islands (50.7°S) during the DEEPWAVE project, *J. Geophys. Res. Atmos.*, 121, 1431–1441, doi:10.1002/2015JD024336.
- Pendleton Jr W.R., Zhao Y., Yuan T., Esplin R., and McLain D., 2014. An Advanced Mesospheric Temperature Mapper for high-latitude airglow studies, *App. Optics*, 53 (26), 5934-5943, doi:10.1364/AO.53.005934.

- Ponthieu, J.J., Killeen, T.L., Lee, K.M., Carignan, G.R., Hoegy, W.R. and Brace, L.H., 1988. Ionosphere-thermosphere momentum coupling at solar maximum and solar minimum from DE-2 and AE-C data. *Physica Scripta*, *37*(3), p.447.
- Prölss, G. W. (1997). Magnetic storm associated perturbations of the upper atmosphere. *Magnetic storms*, 98, 227-241.
- Ridley, A.J., Deng, Y. and Toth, G., 2006. The global ionosphere—thermosphere model. *Journal of Atmospheric and Solar-Terrestrial Physics*, 68(8), pp.839-864.
- Vierinen, J., Chau, J. L., Pfeffer, N., Clahsen, M., and Stober, G., 2016. Coded continuous wave meteor radar, *Atmos. Meas. Tech.*, 9, 829–839, doi: 10.5194/amt-9-829-2016.
- Vierinen, J., Chau, J.L., Charuvil, H., Urco, J.M., Clahsen, M., Avsarkisov, V., Marino, R. and Volz, R., 2019. Observing mesospheric turbulence with specular meteor radars: A novel method for estimating second-order statistics of wind velocity. *Earth and Space Science*, *6*(7), pp.1171-1195.
- Yiğit, E. and Medvedev, A.S., 2012. Gravity waves in the thermosphere during a sudden stratospheric warming. *Geophysical Research Letters*, 39(21).
- Zhang, S.-R., P. J. Erickson, J. C. Foster, J. M. Holt, A. J. Coster, J. J. Makela, J. Noto, J. W. Meriwether, B. J. Harding, J. Riccobono, and R. B. Kerr, 2015. Thermospheric poleward wind surge at midlatitudes during great storm intervals, *Geophys. Res. Lett.*, 42, 5132–5140.
- Zou, S., A. J. Ridley, M. B. Moldwin, M. J. Nicolls, A. J. Coster, E. G. Thomas, and J. M. Rohoniemi, 2013. Multi-instrument observations of SED during 24–25 October 2011 storm: Implications for SED formation processes, *J. Geophys. Res. Space Physics*, 118, 7798–7809, doi:10.1002/2013JA018860.